Transients from initial conditions based on Lagrangian perturbation theory in N-body simulations

Takayuki Tatekawa[†,‡] **and Shuntaro Mizuno**[‖]

†The center for Continuing Professional Development, Kogakuin University, 1-24-2 Nishi-shinjuku, Shinjuku, Tokyo 163-8677, JAPAN

‡Advanced Research Institute for Science and Engineering, Waseda University, 3-4-1 Okubo, Shinjuku, Tokyo 169-8555, JAPAN

‖ Research Center for the Early Universe (RESCEU), School of Science, University of Tokyo, 7-3-1 Hongo, Bunkyo, Tokyo 113-0033, JAPAN

Abstract. We explore the initial conditions for cosmological N-body simulations suitable for calculating the skewness and kurtosis of the density field. In general, the initial conditions based on the perturbation theory (PT) provide incorrect second-order and higher-order growth. These errors implied by the use of the perturbation theory to set up the initial conditions in N-body simulations are called transients. Unless these transients are completely suppressed compared with the dominant growing mode, we can not reproduce the correct evolution of cumulants with orders higher than two, even though there is no problem with the numerical scheme. We investigate the impact of transients on the observable statistical quantities by performing N-body simulations with initial conditions based on Lagrangian perturbation theory (LPT). We show that the effects of transients on the kurtosis from the initial conditions, based on second-order Lagrangian perturbation theory (2LPT) have almost disappeared by $z \sim 5$, as long as the initial conditions are set at $z > 30$. This means that for practical purposes, the initial conditions based on 2LPT are accurate enough for numerical calculations of skewness and kurtosis.

PACS numbers: 02.60.Cb, 02.70.-c, 04.25.-g, 98.65.Dx

1. Introduction

The evolution of the large-scale structure in the Universe is one of the most important topic in astrophysics. The standard scenario for the structure formation is that the primordial density fluctuation grows through its gravitational instability [1, 2, 3, 4, 5]. Even though the perturbative descriptions are possible when the density fluctuation is small enough, in order to follow the distribution far into the nonlinear region, we must, inevitably, rely on the numerical calculations, named, N-body simulations [6].

For N-body simulations, there is a problem about how to set up the initial conditions. Even though the naive expectation is that it is better to start simulations as early as possible, like recombination era, it is well known that this is extremely difficult numerically. When we start N-body simulations at an early era, the initial condition can be overwhelmed by sources of noise, such as the numerical roundoff error or the shot noise of the particles. Therefore, in the standard scheme [7], we must use the perturbative approach. Until the fluctuations come into the quasi-nonlinear regime and stable numerical calculation become possible.

Even though there has been much progress about N-body code with how to solve the non-linear structure in the universe, the method to set up the initial conditions into these codes has been almost the same from the first works of this field [8, 9]. In many cases, the Zel'dovich approximation (ZA) [10], i.e., the first-order approximation of Lagrangian perturbation theory (LPT) have been applied for the initial conditions of N-body simulations for a long time. (For reviews of LPT, see for example [11, 12]). Even though the ZA describe the growth of the density fluctuation much better than the Eulerian linear theory, it does not reproduce the higher order statistics, like skewness and kurtosis with very poor accuracy [13, 14, 15], because the acceleration is always parallel to the peculiar velocity. In other words, the acceleration does not reflect the exact clustering in the ZA.

Therefore, N-body simulations with the ZA initial conditions fail to pick up the correct second- and higher-order growing modes hence failing to reproduce the correct statistical properties of the density fluctuation until very late times [16, 17].

For this problem, recently, Crocce, Pueblas, and Scoccimarro [18] proposed the improvement by adopting different initial conditions. Basically, their initial conditions are based on the approximations valid up to second-order Lagrangian perturbation theory (2LPT) which reproduce exact value of the skewness in the weakly nonlinear region [19, 20]. With these initial conditions, they calculate the statistical quantities and show the effects of transients related with 2LPT initial conditions decrease much faster than the ones related with ZA initial conditions, that is, the transients with 2LPT initial conditions are less harmful than ones with ZA initial conditions.

However, there still exist transients related with 2LPT initial conditions which prevent to reproduce the exact value of higher order statistical quantities like the kurtosis, and there is no guarantee that 2LPT initial conditions are accurate enough for these quantities.

Therefore, as a natural extension of [18], we examine the impact of transients from initial conditions based on 2LPT in N-body simulation. In this paper, in addition to the ZA and 2LPT, we also calculate the non-Gaussianity with the initial conditions based on third-order Lagrangian perturbation theory (3LPT) which reproduce exact value of the kurtosis in the weakly nonlinear region [21, 22, 23, 24, 25].

This paper is organized as follows. In Sec. 2, we present Lagrangian perturbative solutions valid up to the third-order and briefly explain the origin of transients. Then, after introducing the statistical quantities of interest in this paper in Sec. 3, we show the methods and the results of numerical simulations in Sec. 4. For these results, we provide alternative interpretation based on simpler model in Sec. 5. Sec. 6 is devoted to conclusions.

2. Lagrangian perturbations

In this section, we briefly summarize Lagrangian perturbation theory (LPT) and obtain the approximations valid up to the third-order. We also point out explicitly why transients appear in the perturbative approach.

Before considering the perturbation, we present the background cosmic expansion which determines the motion of cosmic fluid in Newtonian cosmology. We consider ΛCDM model in which the Friedmann equations are given as

$$H^2 = \frac{8\pi G}{3}\rho_b + \frac{\Lambda}{3}\,, \tag{1}$$

$$\frac{1}{a}\frac{d^2a}{dt^2} = -\frac{4\pi G}{3}\rho_b + \frac{\Lambda}{3}\,, \tag{2}$$

with a background density ρ_b of pressureless fluid and a cosmological constant Λ.

Even though we take account of Λ for the numerical calculations, we sometimes consider the case with $\Lambda = 0$, so-called Einstein-de Sitter (E-dS) model, for a concrete solution in this section and the next section. This can be justified since the effect of Λ is negligible at the time we set initial conditions for cosmological N- body simulations. For simplicity, in this paper, we do not consider back-reaction from the motion of the matter to cosmic expansion.

Next, we consider the perturbations. In this paper, we consider the Lagrangian perturbation in which solutions for cosmic fluid are already derived by several people [10, 19, 20, 22, 23, 24]. For this purpose, it is necessary to define the comoving Lagrangian coordinates $\boldsymbol{q}$ in terms of the comoving Eulerian coordinates $\boldsymbol{x}$ as:

$$\boldsymbol{q} = \boldsymbol{x} + \boldsymbol{S}(\boldsymbol{x}, t)\,, \tag{3}$$

where $\boldsymbol{S}$ is the displacement vector which denotes the deviation from the homogeneous distribution.

It is worth noting that it is not the density contrast δ but the displacement vector $\boldsymbol{S}$ that is regarded as a perturbative quantity in LPT.

In the Lagrangian coordinates, from the continuous equation, we can express the density contrast exactly as

$$\delta = J^{-1} - 1\,, \tag{4}$$

where J is the determinant of the Jacobian of the mapping between $\boldsymbol{q}$ and $\boldsymbol{x}$: $\partial\boldsymbol{x}/\partial\boldsymbol{q}$. From Eq. (4), we can see that the break down of the perturbation with respect to δ does not necessarily mean that to $\boldsymbol{S}$, which is the strong reason for considering the Lagrangian picture. In other words, although the density diverges or the fluid forms Zel'dovich pancake, the perturbation does not diverge.

From the physical property, $\boldsymbol{S}$ can be decomposed to the longitudinal and the transverse modes:

$$\boldsymbol{S} = \boldsymbol{S}^L + \boldsymbol{S}^T\,, \tag{5}$$

$$\nabla_q \times \boldsymbol{S}^L = 0\,, \tag{6}$$

$$\nabla_q \cdot \boldsymbol{S}^T = 0\,, \tag{7}$$

where ∇_q means the Lagrangian spatial derivative.

In this paper, since it is well known that the transverse mode is negligible for pressureless fluid, we consider only longitudinal mode. From Kelvin circulation theorem, this is quite natural if it is generated only by the action of gravity. For the discussions with the transverse mode in LPT, see [26].

Hereafter we mainly follow the description by Catelan [24]. First, we consider the perturbations in Einstein-de Sitter Universe. In the Lagrangian description, changing the temporal variable as $\tau \equiv t^{-1/3}$, the basic equation for the density contrast for the pressureless fluid named Lagrangian Poisson equation is given by

$$\left[(1 + \nabla_q \cdot \boldsymbol{S})\delta_{\alpha\beta} - S_{\alpha\beta} + S^C_{\alpha\beta}\right] \ddot{S}_{\beta\alpha} = \alpha(\tau)\left[J(\boldsymbol{q},\tau) - 1\right]\,, \tag{8}$$

where $S_{\alpha\beta} \equiv \partial S_\alpha/\partial q_\beta$ is the deformation tensor, $S^C_{\alpha\beta}$ is the cofactor matrix of $S_{\alpha\beta}$. Dots denote the differentiation with respect to τ and $\alpha(\tau)$ is a function of τ which includes the information of cosmic expansion law. Especially for E-dS universe, $\alpha(\tau) = 6\tau^{-2}$.

We now solve the dynamical equations for the displacements $\boldsymbol{S}$ according to the following Lagrangian perturbative prescription:

$$\boldsymbol{S}(\boldsymbol{q},\tau) = \boldsymbol{S}^{(1)}(\boldsymbol{q},\tau) + \boldsymbol{S}^{(2)}(\boldsymbol{q},\tau) + \boldsymbol{S}^{(3)}(\boldsymbol{q},\tau) + \cdots\,. \tag{9}$$

Here $\boldsymbol{S}^{(1)}$ corresponds to the first-order approximation, $\boldsymbol{S}^{(2)}$ to the second-order approximation, and so on. Since we consider only the longitudinal modes, the perturbative solutions are described with gradient of scalar functions,

$$\boldsymbol{S}^{(n)} \equiv \nabla_q S^{(n)}\,. \tag{10}$$

For the pressureless fluid, it can be shown that the perturbative solutions are separable into the temporal and the spatial parts,

$$\boldsymbol{S}^{(1)}(\boldsymbol{q},\tau) = D(\tau)\boldsymbol{s}^{(1)}(\boldsymbol{q})\,, \tag{11}$$

$$\boldsymbol{S}^{(2)}(\boldsymbol{q},\tau) = E(\tau)\boldsymbol{s}^{(2)}(\boldsymbol{q})\,, \tag{12}$$

$$\boldsymbol{S}^{(3)}(\boldsymbol{q},\tau) = F(\tau)\boldsymbol{s}^{(3)}(\boldsymbol{q})\,. \tag{13}$$

The dynamics of the evolution constrains in general both the temporal dependence as described by the functions D, E, F, ... and the spatial displacements $\boldsymbol{s}^{(n)}$.

First we derive the Lagrangian linear perturbative solution (ZA). Making use of the fact that up to the third-order, the following expression for the Jacobian determinant J holds [24]:

$$\begin{aligned} J = 1 &+ \nabla_q \cdot \boldsymbol{S}^{(1)} + \nabla_q \cdot \boldsymbol{S}^{(2)} + \frac{1}{2}\left[(\nabla_q \cdot \boldsymbol{S}^{(1)})^2 - S^{(1)}_{\alpha\beta} S^{(1)}_{\beta\alpha}\right] \\ &+ \nabla_q \cdot \boldsymbol{S}^{(3)} + \left[(\nabla_q \cdot \boldsymbol{S}^{(1)})(\nabla_q \cdot \boldsymbol{S}^{(2)}) - S^{(1)}_{\alpha\beta} S^{(2)}_{\beta\alpha}\right] \\ &+ \det(S^{(1)}_{\alpha\beta})\,, \end{aligned} \tag{14}$$

we can easily find the first-order approximation truncating Eq. (8), which yields,

$$\ddot{D}(\tau) - \alpha(\tau) D(\tau) = 0\,, \tag{15}$$

and no constraint to $\boldsymbol{s}^{(1)}(\boldsymbol{q})$.

For the E-dS model, by substituting $\alpha(\tau) = 6\tau^{-2}$ into Eq. (15), we can obtain the concrete form of the growing mode and the decaying mode solution as

$$D_+(t) = \left(\frac{t}{t_0}\right)^{2/3}\,, \tag{16}$$

$$D_-(t) = \left(\frac{t}{t_0}\right)^{-1}\,. \tag{17}$$

In general, we consider only the growing mode because the decaying mode is suppressed by $a^{-5/2}$ compared to the growing mode and soon becomes negligible.

It is worth noting that the analytic solution for the linear perturbative solution is obtained even in the case with Λ. The perturbative solutions are described as [23]

$$D_+(t) = \frac{h}{2} B_{1/h^2}\left(\frac{5}{6}, \frac{2}{3}\right)\,, \tag{18}$$

$$D_-(t) = h\,, \tag{19}$$

$$h \quad = \sqrt{\frac{3}{\Lambda}}\frac{\dot{a}}{a}\,, \tag{20}$$

where B_{1/h^2} is incomplete Beta function:

$$B_z(\mu,\nu) \equiv \int_0^z p^{\mu-1}(1-p)^{\nu-1}\mathrm{d}p\,. \tag{21}$$

Hereafter we consider growing mode (D_+) only and re-define D as D_+. Even though the impact is not so significant, various modes appear in higher-order perturbation when we consider D_-. For detail, see [27].

Next, we construct the solution valid up to second-order Lagrangian perturbation theory (2LPT). Retaining only the quadratic terms in Eq. (8) and using the first-order results, the system of equations become as follows:

$$\ddot{E}(\tau) - \alpha(\tau) E(\tau) = -\alpha(\tau) D(\tau)^2\,, \tag{22}$$

$$\nabla_q \cdot \boldsymbol{s}^{(2)} = \frac{1}{2}\left[(\nabla \cdot \boldsymbol{s}^{(1)})^2 - s^{(1)}_{\alpha,\beta} s^{(1)}_{\beta,\alpha}\right]\,, \tag{23}$$

where $s_{\alpha,\beta} = \partial s_\alpha / \partial q_\beta$. From Eqs. (22) and (23), we see that unlike the linear case, the second-order approximation constraints both the temporal and the spatial dependence of the solution.

In the E-dS model, by substituting $\alpha(\tau) = 6\tau^{-2}$ into Eq. (22), the growing mode solution can be obtained as

$$E_+(t) = -\frac{3}{7}\left(\frac{t}{t_0}\right)^{4/3} = -\frac{3}{7}D(t)^2\,. \tag{24}$$

In addition to this, the solutions satisfying Eq. (22) without the source term like

$$E_-(t) = c_1 t^{2/3} + c_2 t^{-1}\,, \tag{25}$$

where c_1 and c_2 are constants, also satisfy Eq. (22).

Of course, $E_-(t)$ can be regarded as the "decaying modes" and after some time become negligible regardless of the concrete value of c_1 and c_2 compared to the growing mode $E_+(t)$. They are, however, suppressed by only a^{-1}, and if the initial conditions do not use the exact value for c_1 and c_2, the error survives until late time. These nonphysical decaying modes are well known *transients*.

Actually, if the initial conditions for N-body simulations are set by the ZA, these are appropriate at only linear-order and are inappropriate at second- and higher-order. Therefore, we cannot obtain the correct c_1 and c_2 as long as the initial conditions are set by the ZA. This is the point we discuss in this paper. (For the complete discussions about the origin of transients, see e.g. Sec. 2.1 in [18].)

On the other hand, from Eq. (23) the spatial part can be described as

$$\begin{aligned}\boldsymbol{s}^{(2)} = \frac{1}{2}\left[\boldsymbol{s}^{(1)}\left(\nabla_q\cdot\boldsymbol{s}^{(1)}\right) - \left(\boldsymbol{s}^{(1)}\cdot\nabla_q\right)\boldsymbol{s}^{(1)}\right] \\ + \boldsymbol{R}^{(2)}\,,\end{aligned} \tag{26}$$

where $\boldsymbol{R}^{(2)}$ is a divergence-free vector such that $\nabla_q \times \boldsymbol{s}^{(2)} = 0$.

Then, to see if the effect of transients can be suppressed by considering higher order terms, we continue to analyze the solution valid up to third-order Lagrangian perturbation theory (3LPT). Inserting the expansion Eq. (9) into Lagrangian Poisson equation, and using the results of the linear order and the second-order, we can obtain the third-order expression. It is more convenient to split the third-order displacement $\boldsymbol{S}^{(3)}$ into two parts as follows:

$$\boldsymbol{S}^{(3)}(\boldsymbol{q}) = \boldsymbol{S}_a^{(3)}(\boldsymbol{q}) + \boldsymbol{S}_b^{(3)}(\boldsymbol{q})\,, \tag{27}$$

where $\boldsymbol{S}_a^{(3)}$ is from the cubic interaction among the linear perturbations and $\boldsymbol{S}_b^{(3)}$ is from the interaction between the linear and the second-order perturbations.

Then, the part for $\boldsymbol{S}_a^{(3)}$ is constrained by

$$\ddot{F}_a(\tau) - \alpha(\tau)F_a(\tau) = -2\alpha(\tau)D(\tau)^3\,, \tag{28}$$

$$\nabla_q\cdot\boldsymbol{s}_a^{(3)} = \det(s^{(1)}_{\alpha,\beta})\,. \tag{29}$$

In the E-dS model, by substituting $\alpha(\tau) = 6\tau^{-2}$ into Eq. (28), the growing mode solution can be obtained as

$$F_{a+}(t) = -\frac{1}{3}\left(\frac{t}{t_0}\right)^2 = -\frac{1}{3}D(t)^3\,. \tag{30}$$

In addition to this, the solutions satisfying Eq. (28) without the source term like

$$F_{a-}(t) = c_3 t^{2/3} + c_4 t^{-1}\,, \tag{31}$$

where c_3 and c_4 are constants, also satisfy Eq. (28) and they serve as transients, too, unless the initial condition are set appropriately.

However, compared with the growing mode, these transients are suppressed by a^{-2} and they are less problematic than the transients related to the second-order perturbation, which are suppressed by a^{-1}.

From Eq. (29) we can obtain the spatial part of $\boldsymbol{S}_a^{(3)}$ as

$$s_{a\alpha}^{(3)} = \frac{1}{3}s_{\alpha\beta}^{(1)C}s_{\beta}^{(1)} + R_{a\alpha}^{(3)}\,, \tag{32}$$

where $\boldsymbol{R}_a^{(3)}$ is a divergence-free vector such that $\nabla_q \times \boldsymbol{s}_a^{(3)} = 0$.

On the other hand, the part $\boldsymbol{S}_b^{(3)}$ is constrained by

$$\ddot{F}_b(\tau) - \alpha(\tau)F_b(\tau) = -2\alpha(\tau)D(\tau)[E(\tau) - D(\tau)^2]\,, \tag{33}$$

$$\nabla_q \cdot \boldsymbol{s}_b^{(3)} = \left[(\nabla_q \cdot \boldsymbol{s}^{(1)})(\nabla_q \cdot \boldsymbol{s}^{(2)}) - s_{\alpha,\beta}^{(1)}s_{\beta,\alpha}^{(2)}\right]\,. \tag{34}$$

From the same discussion for the part $\boldsymbol{S}_a^{(3)}$, we can acquire the growing mode solution in the E-dS model,

$$F_{b+}(t) = \frac{10}{21}\left(\frac{t}{t_0}\right)^2 = \frac{10}{21}D(t)^3\,, \tag{35}$$

as well as the spatial part of $\boldsymbol{S}_b^{(3)}$,

$$\begin{aligned}\boldsymbol{s}_b^{(3)} = \frac{1}{4}\big[&\boldsymbol{s}^{(1)}\left(\nabla_q \cdot \boldsymbol{s}^{(2)}\right) - \left(\boldsymbol{s}^{(1)} \cdot \nabla_q\right)\boldsymbol{s}^{(2)} \\ &+\boldsymbol{s}^{(2)}\left(\nabla_q \cdot \boldsymbol{s}^{(1)}\right) - \left(\boldsymbol{s}^{(2)} \cdot \nabla_q\right)\boldsymbol{s}^{(1)}\big] \\ &+ \boldsymbol{R}_B^{(3)}\,,\end{aligned} \tag{36}$$

where $\boldsymbol{R}_b^{(3)}$ is again a divergence-free vector such that $\nabla_q \times \boldsymbol{s}_b^{(3)} = 0$.

3. Statistics

Here, we introduce the statistical quantities of the density fields on which transients provide the impact at large scales. For this purpose, a one-point probability distribution function of the density fluctuation field $P(\delta)$ (PDF of the density fluctuation) which denotes the probability of obtaining the value δ plays an important role. If δ is a random Gaussian field, the PDF of the density fluctuation is determined as

$$P(\delta) = \frac{1}{(2\pi\sigma^2)^{1/2}}e^{-\delta^2/2\sigma^2}\,, \tag{37}$$

where $\sigma^2 \equiv \left\langle (\delta - \langle\delta\rangle)^2 \right\rangle$ is the dispersion and $\langle\ \rangle$ denotes the spatial average.

Since linear growing modes are reproduced almost exactly by the ZA initial condition, the power spectrum, which is the quantity obtained by linear perturbation theory, is not affected by transients. Therefore, the expected tools to detect transients at large scales are the cumulants of the one-point PDF of the density fluctuation field whose orders are higher than two which become nonzero for the distribution deviating from Gaussian. In the structure formation, non-Gaussianity are generated because of the non-linear dynamics of the fluctuations, even though δ is initially treated as a random Gaussian field, as a result of the generic prediction of inflationary scenario.

For this purpose, we concentrate on the third and fourth order cumulants, which are defined as $< \delta^3 >_c \equiv < \delta^3 >$, $< \delta^4 >_c \equiv < \delta^4 > -3\sigma^4$ display asymmetry and non-Gaussian degree of "peakiness", respectively, for a given dispersion [1, 2]. Since it is known that the scaling $< \delta^n >_c \propto \sigma^{2n-2}$ holds for weakly non-linear regions during the gravitational clustering [11] from Gaussian initial conditions, we introduce the following normalized higher-order statistical quantities :

$$\text{skewness} : \gamma = \frac{\langle\delta^3\rangle_c}{\sigma^4}\,,$$
$$\text{kurtosis} \ : \eta = \frac{\langle\delta^4\rangle_c}{\sigma^6}\,.$$

The merit of adopting these definitions is, as stated above, that they are constants in weakly nonlinear stage which are given by Eulerian linear and second-order perturbation theory [1, 11]. For example, in the E-dS model smoothed with a spherical top-hat window function,

$$\tilde{W} = \frac{3(\sin x - x\cos x)}{x^3}\,, \tag{38}$$

the skewness and the kurtosis are given by

$$\gamma = \frac{34}{7} + y_1 + \mathcal{O}(\sigma^2)\,, \tag{39}$$
$$\eta = \frac{60712}{1323} + \frac{62}{3}y_1 - \frac{7}{3}y_1^3 + \frac{2}{3}y_2 + \mathcal{O}(\sigma^2)\,, \tag{40}$$

where

$$y_p \equiv \frac{d^p \ln\sigma^2(R)}{d\ln^p R}, \tag{41}$$

with smoothing scale R [11].

For this form of the skewness and the kurtosis, the effects of transients at large scales from the ZA initial condition is also investigated by [16, 17] as

$$\gamma_{\rm tran} = -\frac{6}{5a} + \frac{12}{35a^{7/2}}\,, \tag{42}$$
$$\eta_{\rm tran} = -\frac{816}{35a} - \frac{28y_1}{5a} + \frac{184}{75a^2} + \frac{1312}{245a^{7/2}} + \frac{8y_1}{5a^{7/2}} - \frac{1504}{4725a^{9/2}} + \frac{192}{1225a^7}\,. \tag{43}$$

For the initial condition, instead of the ZA, if we adopt the one based on 2LPT, transients in the skewness (42) is expected to be vanished at large scales, since 2LPT can provide appropriate initial condition up to second order related with the skewness. Similarly, for the one based on 3LPT, transients in the kurtosis (43) is also expected to be vanished at large scales.

Essentially, in the following section, we examine the effects of transients in the ΛCDM model relying on N-body simulation from the initial conditions based on 2LPT and 3LPT. Since we investigate numerically, we can go into the highly nonlinear region, in which the analytic estimates of transients like Eqs. (42) and (43) can not be performed.

4. Numerical Calculations

In this section, we calculate the statistical quantities introduced in the previous section in the ΛCDM model based on N-body simulations. For setting up the initial conditions, we use COSMICS code [29] which generates primordial Gaussian density field usually based on the ZA. We consider the case with those based on 2LPT and 3LPT, too. COSMICS package consists of 4 applications. GRAFIC generated Gaussian random density fields (density, velocity, and particle displacements) on a lattice. Both the velocity and the displacements are related to each other.

GRAFIC automatically selects the output redshift by the maximum density fluctuation on a grid δ_{max} for a given set of cosmological parameters. In order to obtain the initial redshift, we adopt the following cosmological parameters at the present time ($z = 0$) which are given by WMAP 3-year result [30]:

$$\Omega_m = 0.28\,, \tag{44}$$

$$\Omega_\Lambda = 0.72\,, \tag{45}$$

$$H_0 = 73\ [\mathrm{km/s/Mpc}]\,, \tag{46}$$

$$\sigma_8 = 0.74\,. \tag{47}$$

The averaged relation between the input maximum density fluctuation and the output redshift is shown in Table. 1. The initial redshift is set by the input maximum density fluctuation. Because we set random Gaussian fluctuation, the initial redshift is not fixed.

From the initial conditions set up above, we follow the evolution of the particles based on N-body simulation. The numerical algorithm is applied by particle-particle particle-mesh (P^3M) method [6] which was developed by Gelb and Bertschinger. The numerical code we use is written by Bertschinger. For N-body simulations, we set the parameters as follows:

$$\begin{aligned}
&\text{Number of particles} : N = 128^3\,,\\
&\text{Box size} \qquad\qquad : L = 128h^{-1}\mathrm{Mpc}\ \ (\text{at } z = 0)\,,\\
&\text{Softening length} \quad : \varepsilon = 50h^{-1}\mathrm{kpc}\ \ (\text{at } z = 0)\,.
\end{aligned}$$

Table 1. The averaged redshift and its dispersion of the initial condition selected by the GRAFIC code for a given maximum density fluctuation.

δ_{max}	$\bar{z}$	σ_z
1.0	22.821	0.868
0.5	32.833	1.670
0.2	83.806	4.256

For the simulations, we use 50 samples for an initial condition. After the calculations, in order to avoid the divergence of the density fluctuation in the limit of large k, however, just for a technical reason, it is necessary to consider the density field $\rho_m(\boldsymbol{x}; R)$ at the position $\boldsymbol{x}$ smoothed over the scale R, which is related to the unsmoothed density field $\rho_m(\boldsymbol{x})$ as

$$\rho_m(\boldsymbol{x}; R) = \int d^3\boldsymbol{y} W(|\boldsymbol{x} - \boldsymbol{y}|; R)\rho_m(\boldsymbol{y}) \,, \tag{48}$$

where we use the top-hat spherical window function by Eq. (38). Throughout this paper, we choose the smoothing scale $R = 2h^{-1}$Mpc (at $z = 0$).

Crocce, Pueblas, and Scoccimarro [18] analyzed the non-Gaussianity of the density field with both the skewness and the kurtosis. They changed the smoothing scale R and compared the non-Gaussianity with two different initial conditions which are based on the ZA and 2LPT, respectively. Then they showed that the difference of the skewness and the kurtosis for $R = 2h^{-1}$ Mpc becomes several percent at $z = 0$, when the initial condition is imposed at $z = 24$.

Here, in addition to the ZA and 2LPT, we also analyze the non-Gaussianity with the initial conditions based on 3LPT, by slightly modifying the COSMICS so that initial conditions are set up by not only the ZA but also 2LPT and 3LPT. Using output files which describe the ZA displacement from COSMICS, we compute 2LPT and 3LPT displacements and velocities using Eqs. (26), (32), and (36). Here we set $\boldsymbol{R}^{(2)} = \boldsymbol{R}_A^{(3)} = \boldsymbol{R}_B^{(3)} = \boldsymbol{0}$. The vectors $\boldsymbol{R}^{(2)}, \boldsymbol{R}_A^{(3)}$, and $\boldsymbol{R}_B^{(3)}$ were introduced for rotation-free condition. Because we set these vectors as zero, the rotation-free condition slightly violates.

The main purpose is to see the impacts of transients from 2LPT initial conditions since 3LPT initial conditions are expected to provide exact results for the kurtosis. We investigate this also by changing the initial time dependence which corresponds to the initial maximum density fluctuation for a given Fourier mode. We expect this can clarify the range where N-body simulations from 2LPT initial conditions are accurate enough.

First, we analyze the case in which the initial condition is imposed after the density fluctuation becomes relatively large ($\delta_{max}(t_i) = 1$).

Before analyzing the non-Gaussianity, we consider the evolution of the dispersion of the density distribution (Fig. 1). We can see that the ZA is a good approximation initially, but it gradually deviates from the one from 2LPT initial condition because of the nonlinear effects. The final difference between the dispersions with the initial

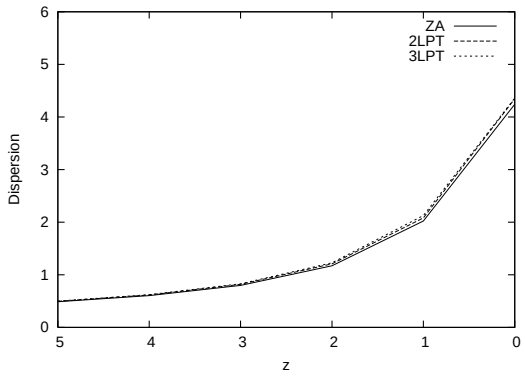

Figure 1. The dispersion of the density distribution from N-body simulation ($R = 2h^{-1}$ Mpc) with different initial conditions. The difference between dispersion with the initial conditions based on the ZA and 3LPT is less than 4% at $z = 0$.

conditions based on the ZA and 2LPT is less than 4%. There is almost no difference between the dispersions in density with the initial conditions based on 2LPT and 3LPT. Obviously, this confirms the strength of ZA, that can reproduce the growth of the density fluctuations well within the quasi-nonlinear regime.

However we also see that when it comes to the non-Gaussianity which include the skewness and higher-order moments, the validity of the ZA is very limited (Fig. 2). The difference between the skewness and the kurtosis with the initial conditions based on the ZA and 3LPT become about as much as 15% and 40% (at $z = 2$), respectively. Furthermore, the difference between them based on 2LPT and 3LPT becomes also significant. This means that the simulations with the initial condition based on 2LPT does not provide the correct skewness because nonlinearity at this initial time is significant. Without doubt, in such a case in which the initial condition is imposed at $z \simeq 23$ like [18], it is not enough to consider the initial condition based on 2LPT and we can acquire much more accurate values with the initial condition based on 3LPT.

Next, we analyze the cases in which initial conditions are imposed for smaller density fluctuations. We reduce the maximum value of the density fluctuation $\delta_{max}(t_i)$ at initial time to 0.5, and 0.2. Decreasing δ_{max} will lead to less analytically evolved solutions and more numerical evolution and hence is expected to decrease the effect of transients which are due to analytical evolution. For the case $\delta_{max}(t_i) = 0.5$, we can see that the difference between the non-Gaussianity with the initial conditions based on the ZA and 3LPT is much smaller than the case $\delta_{max}(t_i) = 1.0$ (Fig. 3). This is because for the smaller density fluctuation, the higher order effect in LPT becomes less efficient and the ZA is better approximation for the initial condition. We can also see that the non-Gaussianity with the initial condition based on the ZA approaches those with the initial condition based on 2LPT and 3LPT at late time. This means that transients disappear until that.

It is worth noting here is that for $\delta_{max}(t_i) = 0.5$, there is no difference between the skewness with the initial conditions based on 2LPT and 3LPT since even 2LPT provides

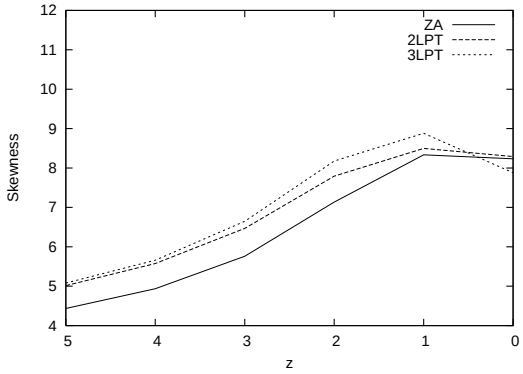

(a)

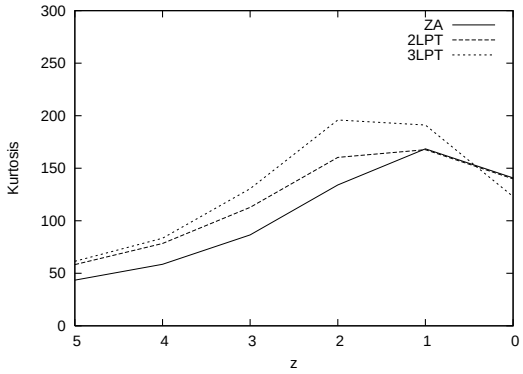

(b)

Figure 2. The non-Gaussianity of the density distribution from N-body simulation ($\delta_{max}(t_i) = 1.0, R = 2h^{-1}$ Mpc) with different initial conditions. (a) The skewness of the density distribution. The difference between the skewness with the initial conditions based on the ZA and 3LPT is less than 14%. Furthermore, the skewness with the initial condition based on 2LPT does not coincide with that based on 3LPT obviously because of the high nonlinearity of the initial time. (b) The kurtosis of the density distribution. The difference between the kurtosis with the initial conditions based on ZA and 3LPT is less than 40%. Furthermore, the kurtosis with the initial condition based on 2LPT does not coincide with that based on 3LPT obviously.

accurate skewness for this initial time with small nonlinearity. For the kurtosis, the difference with the initial conditions based on 2LPT and 3LPT is also very small (at most less than 2%), because transients with 2LPT decreases faster than that with the ZA. This difference disappears until late time as the transients vanishes at that time.

Furthermore, we examine the case $\delta_{max}(t_i) = 0.2$ (Figs. 4). Both of the cases, the difference between the non-Gaussianity with the initial conditions based on 2LPT and 3LPT almost disappears, as is expected from the results of the case $\delta_{max}(t_i) = 0.5$. Even for the kurtosis, we cannot see the difference because before $z = 5$, transients with 2LPT completely disappear.

What is quantitatively important here is that the difference between the skewness and the kurtosis of the density distribution with the initial conditions based on the ZA

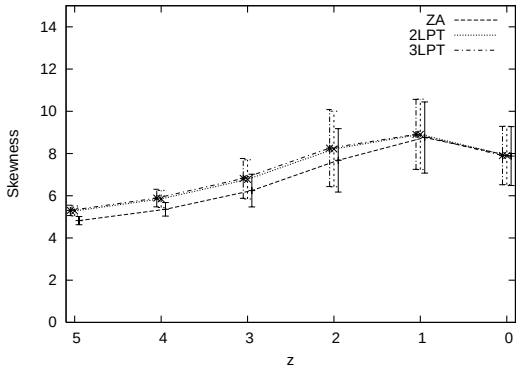

(a)

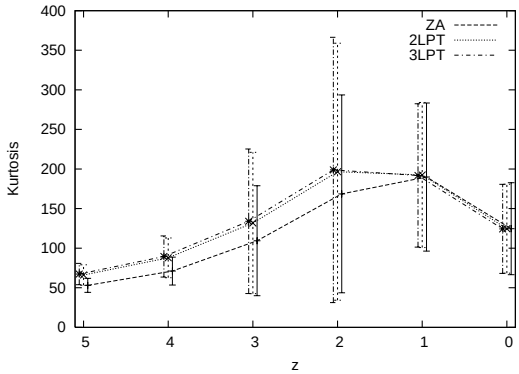

(b)

Figure 3. The non-Gaussianity of the density distribution from N-body simulation ($\delta_{max}(t_i) = 0.5, R = 2h^{-1}$ Mpc) with different initial conditions. we also show the error bars. (a) The skewness of the density distribution. The difference between the skewness with the initial conditions based on the ZA and 3LPT is less than 10%. Because of the suppressions of transients at late time, this difference disappears at late time. Notice that there is no difference between the skewness with the initial conditions based on 2LPT and 3LPT since 2LPT provides almost exact skewness for this initial time with small nonlinearity. (b) The kurtosis of the density distribution. The difference between the kurtosis with the initial conditions based on the ZA and 3LPT is less than 25%. Because of the suppressions of transients at late time, this difference disappears at late time. Notice that the difference between the kurtosis with the initial conditions based on 2LPT and 3LPT is less than 2% and almost disappears at late time because transients with 2LPT decrease much faster than the one with the ZA.

and 2LPT still survives for such a small value of $\delta_{max}(t_i) = 0.2$ until $z \sim 1$. This means that it takes a long time for transients with the ZA to completely disappear.

By now, we only show the results after $z = 5$, even though we have actually done the numerical calculations from about $z = 20$. For the reader who are interested in the thorough evolution of the statistical quantities, we show one example with $\delta_{max}(t_i) = 0.5$ (Fig. 5).

To finish this section, it is worth commenting on the error bars in the curves (Fig 3).

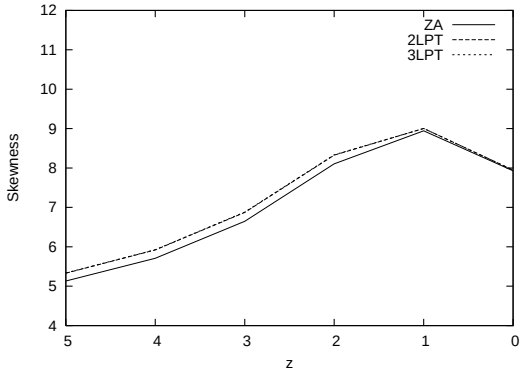

(a)

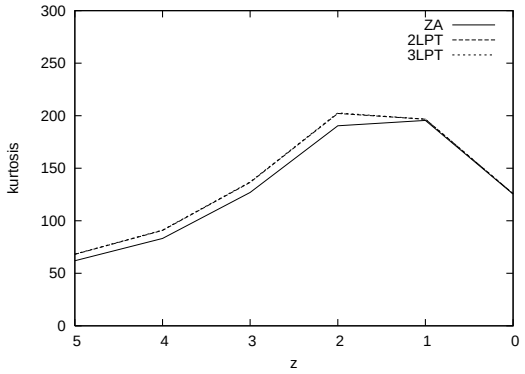

(b)

Figure 4. The non-Gaussianity of the density distribution from N-body simulation ($\delta_{max}(t_i) = 0.2, R = 2h^{-1}$ Mpc) with different initial conditions. (a) The skewness of the density distribution. There is no difference between the skewness with the initial conditions based on 2LPT and 3LPT since 2LPT provides almost exact skewness for this initial time with small nonlinearity. The difference between the skewness with the initial conditions based on the ZA and 2LPT is less than 4% but remains until $z \sim 1$ because of transients. (b) The kurtosis of the density distribution. The difference between the kurtosis with the initial conditions based on 2LPT and 3LPT become negligible because transients with 2LPT have disappeared until $z \sim 5$. The difference between the kurtosiss with the initial conditions based on the ZA and 2LPT is less than 10% but remains until $z \sim 1$ because of transients.

Although we only show error bars the $\delta_{max}(t_i) = 0.5$ case, their values are almost independent of the initial conditions (ZA, 2LPT or 3LPT), hence hold for the other simulations. In Table 2 and Table 3, we show the concrete values for the errors.

5. Nonlinear effects in top-hat spherical symmetric model

According to the numerical calculation in the previous section, we see that even though the difference between the non-Gaussianity with the initial conditions based on the ZA and 2LPT can not be removed well by taking the initial time at sufficiently high-z era, it can be significantly decreased between those based on 2LPT and 3LPT. Especially,

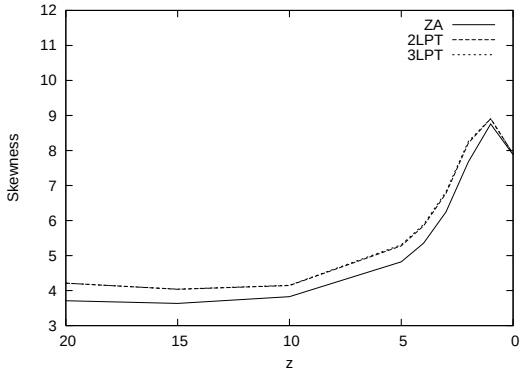

(a)

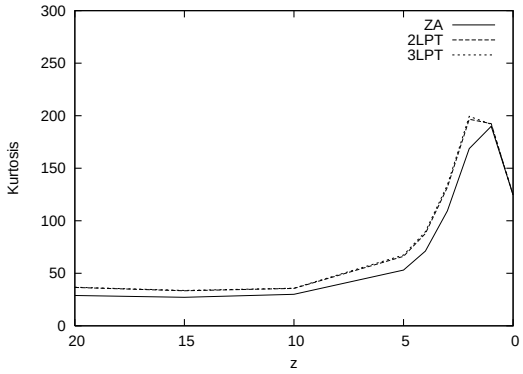

(b)

Figure 5. The non-Gaussianity of the density distribution from N-body simulation ($\delta_{max}(t_i) = 0.5, R = 2h^{-1}$ Mpc) with different initial conditions. They are based on the same calculation as in Fig. 3, but show the evolution of the statistical quantities from $z = 20$. (a) The skewness of the density distribution. (b) The kurtosis of the density distribution.

Table 2. The error of the statistical quantities at $z = 2$ from N-body simulation ($\delta_{max}(t_i) = 0.5, R = 2h^{-1}$ Mpc) with different initial conditions.

Initial condition	Dispersion	Skewness	Kurtosis
ZA	3.2%	19.6%	74.1%
2LPT	3.4%	21.8%	82.6%
3LPT	3.5%	22.1%	84.3%

the difference between the kurtosis which initially includes transients with 2LPT has disappeared until $z \sim 2$, if we set the initial time for N-body simulation around $z \sim 33$ (Table 1).

For the interpretation and further analytical justification for the results, in this section, we reconsider a simpler situation modeled by a top-hat spherical symmetric collapse with constant density for which both the exact solution and Lagrangian perturbative expansion are obtained analytically [12, 21, 25]. Another motivation

Table 3. The error of the statistical quantities at $z = 0$ from N-body simulation ($\delta_{max}(t_i) = 0.5, R = 2h^{-1}$ Mpc) with different initial conditions.

Initial condition	Dispersion	Skewness	Kurtosis
ZA	6.9%	17.8%	46.6%
2LPT	7.0%	17.5%	45.1%
3LPT	7.0%	17.5%	45.2%

for the symmetric collapse, is that it provides most severe constraints for Lagrangian perturbation theory, in general, as shown by Yoshisato *et al.* [31].

In this section, we reset the definition of the scale factor a. If such a shell is in the Einstein-de Sitter universe, the equation of motion for a spherical shell is given by

$$\frac{d}{dt}\left(a^2\frac{dx}{dt}\right) = -\frac{2a^2x}{9t^2}\left[\left(\frac{x_0}{x}\right)^3 - 1\right], \tag{49}$$

where $a(t) \propto t^{2/3}$ is a scale factor, x is a comoving radial coordinate and $x_0 = x(t_0)$. For the derivation of Eq. (49), see around Eq. (17) in [21].

Under the initial condition $\delta = a$ for $a \to 0$, Eq. (49) can be integrated as,

$$\left(\frac{dR}{da}\right)^2 = a\left(\frac{1}{R} - \frac{3}{5}\right), \tag{50}$$

where $R(t) = a(t)x/x_0$ is a physical particle trajectory. It is known that the exact solution for the spherical collapse (Eq. (50)) can be parametrized as follows:

$$R(\theta) = \frac{3}{10}(1 - \cos\theta), \tag{51}$$

$$a(\theta) = \frac{3}{5}\left[\frac{3}{4}(\theta - \sin\theta)\right]^{2/3}. \tag{52}$$

From Eqs. (51) and (52), we can also obtain the density contrast given by $\delta \equiv (x_0/x)^3 - 1$ as [12, 21, 25],

$$\delta(x) = \frac{9(\theta - \sin\theta)^2}{2(1 - \cos\theta)^3} - 1\,. \tag{53}$$

Together with Eqs. (52), (53) and the definition of the density contrast, we can express $R(t)$ exactly in terms of the function $a(t)$.

Obviously, this exact expression can be expanded in terms of a like

$$R(t) = R_0\left[1 - \sum_{k=1}^{n}(-1)^k C_k a^k\right], \tag{54}$$

where C_k are perturbative coefficients. It can be shown that the first three terms of this expansion are given as

$$C_1 = \frac{1}{3}, \quad C_2 = \frac{1}{21}, \quad C_3 = \frac{23}{1701}\,. \tag{55}$$

Since Eq. (54) is an expansion with respect to the displacement from the homogeneous distribution, this is nothing but the Lagrangian perturbation.

On the other hand, for a general symmetric spherical symmetric collapse, the density fluctuation in Eulerian picture at r can be related with the perturbation variable in Lagrangian picture as follows:

$$\delta(r) = \left(1 - \frac{\partial}{\partial r} s(r)\right)^{-3} - 1\,, \tag{56}$$

where $s(r)$ means the radial component of Lagrangian displacement which can be expanded as

$$s(r) = s^{(1)}(r) + s^{(2)}(r) + s^{(3)}(r) + O(\varepsilon^4)\,. \tag{57}$$

Compared with Eq. (54) and Eq. (56) together with the definition of the density contrast, we can obtain the following relations:

$$\frac{\partial s}{\partial r} = \sum_{k=1}^{n} (-1)^k C_k a^k\,, \tag{58}$$

and applying the expansion given by Eq. (57) this yields

$$\frac{\partial}{\partial r} s^{(1)}(r) = \frac{1}{3} a, \tag{59}$$

$$\frac{\partial}{\partial r} s^{(2)}(r) = \frac{1}{21} a^2 = \frac{3}{7} \left(\frac{\partial}{\partial r} s^{(1)}(r)\right)^2\,, \tag{60}$$

$$\frac{\partial}{\partial r} s^{(3)}(r) = \frac{23}{1701} a^3 = \frac{23}{63} \left(\frac{\partial}{\partial r} s^{(1)}(r)\right)^3\,. \tag{61}$$

This spherical model forms caustics at $a = 3$ in the ZA. Here we note that this is an ideal model, and the value of a which forms caustics is different from the actual Universe.

In GRAFIC code, the initial conditions are automatically set when the maximum density fluctuation at any lattice point becomes greater than some value. If the point is approximated as the center of the spherical collapse, we can derive the relation between the density fluctuation and the linear Lagrangian displacements from Eq. (56).

$$\frac{\partial}{\partial r} s^{(1)}(r) = 1 - (1 + \delta(r))^{-1/3}\,. \tag{62}$$

The linear Lagrangian displacements at this time becomes

$$\frac{\partial}{\partial r} s^{(1)}(r) \simeq 0.206299 \quad \text{for } \delta = 1, \tag{63}$$

$$\frac{\partial}{\partial r} s^{(1)}(r) \simeq 0.126420 \quad \text{for } \delta = 0.5, \tag{64}$$

$$\frac{\partial}{\partial r} s^{(1)}(r) \simeq 0.058964 \quad \text{for } \delta = 0.2\,. \tag{65}$$

Therefore based on the discussions in this section, we can calculate the effect of 2LPT and 3LPT at initial time (Table 4).

Here we regard the actual Universe with the above result. Clearly, by regarding the top-hat spherical collapse considered in this section as the generation of the overdense regions through gravitational instability in the Universe, this analysis provides another explanation for the results in the previous section. For example, for the initial condition

Table 4. The effect of the second- and third-order perturbation for the density fluctuation evaluated at a given δ during the top-hat spherically symmetric collapse. $\delta^{(i)}$ denotes that this quantity is calculated by $i-$th order Lagrangian perturbation theory.

δ	$\delta^{(2)}/(\delta^{(1)}+\delta^{(2)})$	$\delta^{(3)}/(\delta^{(1)}+\delta^{(2)}+\delta^{(3)})$
1.0	14.4%	2.34%
0.5	7.17%	0.73%
0.2	2.86%	0.14%

$\delta_{max}=1$, the effect of 3LPT has become significant, while for $\delta_{max}=0.5$ and $\delta_{max}=0.2$ it is only below 1% and eventually negligible. On the other hand, the effect of 2LPT is still significant even we choose the initial condition with smaller density fluctuation like $\delta_{max}=0.2$.

6. Summary

Recently, observations have improved the precision of cosmological constraints tremendously. In order to compare theoretical predictions with observational results, we should carry out detailed numerical simulations with high accuracy. In this context, in order to follow the nonlinear evolution, one needs to consider carefully how to set initial conditions of N-body simulations very carefully. In the standard method, the initial conditions are set up by the Zel'dovich approximation (ZA) in the quasi-nonlinear regime. The ZA has the nice property that by using linear perturbation theory allows one to describe accurately the quasi-nonlinear density field, in the case of small non-linearity.

On the other hand, when constraining cosmological models, non-Gaussianity of the density fluctuations generated by the nonlinear dynamics will become important. It is well known that the ZA is not sufficient to measure non-Gaussianity from higher-order statistics, for example, the skewness and kurtosis. The reason is the existence of so-called transients, that is, the most dominant decaying mode arising from our ignorance of the initial conditions. Until the effects of transients have disappeared, we can not accurately reproduce higher-order quantities like the skewness and the kurtosis.

Actually, recently, Crocce, Pueblas, and Scoccimarro [18] analyzed the impact of transient on the second- and higher-order statistics quantitatively for N-body simulations by comparing the initial conditions based on the ZA and second-order Lagrangian perturbation theory (2LPT). They show that even though there are also transients from 2LPT initial conditions, the effects of transients are suppressed compared to the ZA case.

In this paper, as a natural extension of [18], in addition to the ZA and 2LPT, we also analyze the non-Gaussianity with the initial conditions based on third-order Lagrangian perturbation theory (3LPT). Since 3LPT initial conditions are expected to provide exact results for the kurtosis in the weakly nonlinear region, we can evaluate

the impact of transients from 2LPT initial conditions. The goal is to clarify the range where N-body simulations from 2LPT initial conditions are accurate.

When we set the initial condition of the maximal density contrast reaching unity ($\delta_{max} \sim 1$) at $z \simeq 20$, differences in the predicted non-Gaussianity between the three different initial conditions (ZA, 2LPT and 3LPT) are readily apparent. Since the accurate value of the skewness is reproduced by 2LPT for the weakly nonlinear regime, this disagreement is because of the nonlinearity at this initial time. Therefore, 2LPT initial conditions are not sufficient to set up the initial condition for N-body simulations. There is also no guarantee that 3LPT initial conditions are accurate enough for precise determination of cosmological parameters.

Next, to avoid the problem with the initial nonlinearity, we set the initial conditions at $z \simeq 30$, corresponding to the maximal density contrast is about half, ($\delta_{max} \sim 0.5$). In this case, as is expected from the predictions of 2LPT in the weakly nonlinear region, we find no difference between the 2LPT and 3LPT results, confirming that the 2LPT initial conditions produce accurate skewness. For the kurtosis, the difference between the initial conditions with 2LPT and 3LPT is also very small (2%). On the other hand, the difference of non-Gaussianity with initial conditions based on the ZA and 3LPT is large (10% for the skewness and 25% for the kurtosis) until $z \sim 1$. This shows that transients from initial conditions with 2LPT have less impact than the ones with the ZA initial conditions.

This tendency is also obtained for the initial conditions set at $z \simeq 80$ when the maximal density contrast is about two-tenths, ($\delta_{max} \sim 0.2$). From the numerical calculations for the kurtosis, we can see that the effects of transients from 2LPT initial condition have completely disappeared until $z \sim 5$. However, there is still significant differences in the predicted non-Gaussianity with initial conditions based on the ZA and 3LPT (4% for the skewness and 10% for the kurtosis) until $z \sim 1$.

Therefore, for sufficiently early $z > 30$ initial conditions, the effects of transients on kurtosis from 2LPT initial conditions become negligible until roughly $z \sim 3$, while those from the ZA initial conditions survive until $z \sim 1$. As long as one considers typical N-body simulations, which start at $z \sim 50$, the predicted statistics are accurate enough up to the forth-order (kurtosis) using 2LPT initial conditions.

We further investigated our above results semi-analytically by considering the simpler situation modeled by a top-hat spherically symmetric collapse with constant density. We can show that in this situation, the difference between the impact of 2LPT and 3LPT initial conditions becomes almost negligible for the initial maximum density contrast much less than the half ($\delta_{max} \sim 0.5$), while the difference between the impact of the ZA and 2LPT initial conditions is still greater than 2% for the initial maximum density contrast about two-tenth ($\delta_{max} \sim 0.2$).

Finally, we briefly mention the observational consequences of our results. It is known that weak lensing surveys can potentially provide us with precision maps of the projected density up to redshifts around 1 [32, 33, 34, 35, 36]. Even though we need another step in obtaining the convergence field which can be written as the projection of

the matter density along the line of sight, the skewness and kurtosis of the convergence field can be tested via weak lensing surveys. Our comparison of the initial conditions should prove useful extracting cosmological parameters from observational data.

Acknowledgments

SM is supported by JSPS. We thank Masahiro Morikawa and Shoichi Yamada for useful comments. We are grateful to Erik Reese for checking of English writing of this paper.

References

[1] Peebles P J E 1980 *The Large-Scale Structure of the Universe* (Princeton: Princeton University Press)
[2] Peacock J 1999 *Cosmological Physics* (Cambridge: Cambridge University Press)
[3] Liddle A R and Lyth D H 2000 *Cosmological Inflation and Large-Scale Structure* (Cambridge: Cambridge University Press)
[4] Coles P and Lucchin F 2002 *Cosmology, The Origin and Evolution of Cosmic Structure* (Chichester: John Wiley)
[5] Sahni V and Coles P 1995 *Phys. Rep.* **262** 1
[6] Hockney W R and Eastwood W 1981 *Computer Simulation Using Particles* New York: (McGraw-Hill); Bertschinger E and Gelb J M 1991 *Computers in Physics* **5** (2) 164
[7] Bertschinger E 1998 *Ann. Rev. Astron. Astrophys.* **36** 599
[8] Klypin A and Shandarin S F 1983 *Mon. Not. R. Astron. Soc.* **204** 891
[9] Efstathiou G, Davis M, Frenk C S and White S D M 1985 *Astrophys. J. Suppl.* **57** 241
[10] Zel'dovich Ya B 1970 *Astron. Astrophys.* **5** 84
[11] Bernardeau F, Colombi S, Gaztañaga E and Scoccimarro R 2002 *Phys. Rept.* **367**, 1
[12] Tatekawa T 2005 *Recent Res. Devel. Astrophys.* **2** 1 [arXiv:astro-ph/0412025].
[13] Juszkiewicz R, Bouchet F R and Colombi S 1993 *Astrophys. J.* **412** L9 [arXiv:astro-ph/9306003].
[14] Juszkiewicz R, Weinberg D H, Amsterdamski P, Chodorowski M and Bouchet F 1995 *Astrophys. J.* **442** 39
[15] Baugh C M, Gaztanaga E and Efstathiou G 1995 *Mon. Not. Roy. Astron. Soc.* **274** 1049
[16] Scoccimarro R 1998 *Mon. Not. Roy. Astron. Soc.* **299** 1097 [arXiv:astro-ph/9711187].
[17] Valageas P 2002 *Astron. Astrophys.* **385** 761
[18] Crocce M, Pueblas S and Scoccimarro R 2006 *Mon. Not. R. Astron. Soc.* **373** 369
[19] Bouchet F R, Juszkiewicz R, Colombi S and Pellat R 1992 *Astrophys. J.* **394** L5
[20] Buchert T and Ehlers J 1993 *Mon. Not. R. Astron. Soc.* **264** 375
[21] Munshi D, Sahni V and Starobinsky A A 1994 *Astrophys. J.* **436** 517 [arXiv:astro-ph/9402065].
[22] Buchert T 1994 *Mon. Not. R. Astron. Soc.* **267** 811
[23] Bouchet F R, Colombi S, Hivon E, and Juszkiewicz R, *Astron. Astrophys.* **296** 575
[24] Catelan P 1995 *Mon. Not. R. Astron. Soc.* **276** 115
[25] Sahni V and Shandarin S F 1996 *Mon. Not. Roy. Astron. Soc.* **282** 641 [arXiv:astro-ph/9510142].
[26] Strictly speaking, even if we ignore pressure of fluid, it is shown that third-order transverse mode appears [27], in principle. In generic cases, however, the effect of the third-order transverse mode is quite small quantitatively. Furthermore, if we consider special situations when the fluid affects some kind of pressure gradient, transverse mode appears from the second-order [28].
[27] Sasaki M and Kasai M 1998 *Prog. Theor. Phys.* **99** 585
[28] Morita M and Tatekawa T 2001 *Mon. Not. R. Astron. Soc.* **328** 815; Tatekawa T *et al.* 2002 *Phys. Rev. D* **66** 064014; Tatekawa T 2005 *Phys. Rev. D* **72** 024005
[29] Ma C P and Bertschinger E 1995 *Astrophys. J.* **455** 7

[30] Spergel D N *et al.*, astro-ph/0603449.
[31] Yoshisato A, Morikawa M, Gouda N and Mouri H 2006 *Astrophys. J.* **637** 555 [arXiv:astro-ph/0510107].
[32] van Waerbeke L *et al.* 2000 *Astron. Astrophys.* **358** 30 [arXiv:astro-ph/0002500].
[33] Bacon D J, Refregier A R and Ellis R S 2000 *Mon. Not. Roy. Astron. Soc.* **318** 625 [arXiv:astro-ph/0003008].
[34] Wittman D M, Tyson J A, Kirkman D, Dell'Antonio I and Bernstein G 2000 *Nature* **405** 143 [arXiv:astro-ph/0003014].
[35] Kaiser N, Wilson G and Luppino G A, [arXiv:astro-ph/0003338].
[36] Huterer D and Takada M 2005 *Astropart. Phys.* **23** 369 [arXiv:astro-ph/0412142].